Mechanistic dissection of a dopamine-gated cation channel from *Daphnia* reveals key determinants of ligand selectivity and sensitivity

Tina M. McRunnel[1], Thomas E. Reynoldson[1], Iris Hardege[1*]

1. Department of Zoology, University of Cambridge, UK
* Corresponding author

Abstract

The pentameric ligand-gated ion channels (pLGICs) are a deeply conserved superfamily that includes nicotinic acetylcholine (nAChR), $GABA_A$Rs, glycine, and serotonin receptors and mediates fast neurotransmission. While vertebrate pLGICs have been extensively characterized, recent discoveries in invertebrates have revealed atypical members with novel ligand specificities, including dopamine-gated ion channels (dop-LGICs) that enable direct ionotropic dopaminergic signaling. Here, we investigate the molecular determinants of catecholamine sensitivity and selectivity in a cation-permeable dopamine-gated receptor from *Daphnia magna* (Dm-DopC1), which shares high structural homology with vertebrate nAChRs. We find that mutations in loop B (D188N) near-abolish catecholamine responses, while substitutions in loops A (S123P) and C (S227G, E230P) significantly alter sensitivity and ligand selectivity, highlighting the cooperative role of these loops in shaping receptor pharmacology. Complementary face mutations in loops D and E (N92T, A158G) further refined dopamine versus norepinephrine sensitivity. Finally, we also show that this dopamine receptor can be antagonized by both nicotinic and dopaminergic compounds, underscoring its hybrid pharmacological profile. Together, these results reveal how subtle changes in conserved binding motifs can shift receptor specificity from cholinergic to dopaminergic signaling, providing new insights into the evolutionary flexibility of pLGICs and the molecular basis of ionotropic catecholamine transmission in invertebrates.

1. Introduction

The processes governing neural communication are dynamic and highly evolutionarily conserved in animals across phyla (Moroz et al., 2021). Relying on the highly orchestrated molecular mechanisms that mediate the release and detection of neurotransmitters, converting extracellular chemical cues into either rapid electrical shifts in cell membrane potential or slower intracellular signaling cascades. Neurotransmission occurs via two distinct pathways: ionotropic and metabotropic. Ionotropic receptors, mediate fast synaptic transmission while in contrast, metabotropic receptors act through slow and second messenger pathways and produce longer lasting, modulatory effects.

The most widespread ionotropic receptors in animals fall into the pentameric or Cys-loop ligand gated ion channel superfamily (pLGIC), which includes nicotinic acetylcholine receptors (nAChR), $GABA_A$ receptors, glycine receptors (GlyR) and serotonin receptors ($5HT_3R$), each typically associated with distinct neurotransmitters and ionic conductances. The structural architecture of pLGICs is highly conserved and consists of five subunits arranged symmetrically around a central ion pore (Figure 1A). Each subunit contributes a β-sandwich extracellular domain (ECD) and four transmembrane α-helices. Neurotransmitter binding occurs at the interfaces between subunits, where on subunit serves as the 'principal face' contributing three extracellular loops A-C and the other contributes loops D-F to form a composite ligand binding site (Figure 1B) (Lynagh and Pless, 2014). While some pLGICs function as homomers most receptors are formed of heteromeric combinations of up to 5 different subunits (Boulin et al., 2008) with the ligand binding interface only forming between specific subunit combinations. Despite this conserved scaffold, structural studies have revealed how small differences in loop composition and conformation underlie substantial diversity in ligand recognition and receptor pharmacology (Corringer et al., 2010; Dalal et al., 2025; Dani, 2015; Pan et al., 2012; Sauguet et al., 2014; Unwin, 2003). This class of receptors have been extensively studied in vertebrate systems, and these receptors have become major pharmacological targets, forming the basis of anesthetics, antiparasitic and anxiolytics. This vertebrate-centric knowledge base has shaped much of our understanding of synaptic transmission. However, studies in invertebrate models have uncovered atypical pLGICs with unexpected ligand specificity, gating properties and synaptic roles (Cully et al., 1996; Ringstad et al., 2009). Characterizing these divergent receptors is essential for understanding the evolutionary diversity and functional plasticity possible in neurotransmission. For example, it was once assumed that each neurotransmitter exerts either an excitatory or an inhibitory effect depending on the receptor class that it activates. However, the discovery of both excitatory and inhibitory glutamate-gated chloride channels (GluCls) in *Caenorhabditis elegans* and *Drosophila melanogaster* challenged this view (Cully et al., 1996, 1994). These invertebrate-

specific channels are the targets for the antiparasitic treatment ivermectin, which locks the channel in an open state, causing paralysis in parasitic worms.

One of the most intriguing discoveries in invertebrate systems is the identification of ligand-gated ion channels gated by dopamine (dop-LGICs), which enable direct, ionotropic dopaminergic signalling (Courtney et al., 2025; Morud et al., 2021; Ringstad et al., 2009). This mode of neurotransmission contrasts with canonical dopaminergic signalling in mammals, which is mediated by GPCRs. The most recently identified cation permeable dop-LGIC which is gated by the catecholamines dopamine, norepinephrine and epinephrine has been shown to be conserved in multiple invertebrate species, including *Daphnia magna, Apis mellifera*, *Aplysia california* and *Octopus sinensis* (Courtney et al., 2025). In contrast, the anion dop-LGICs studied previously appear to be nematode specific and gated by dopamine and to a lesser extent tyramine (Morud et al., 2021; Ringstad et al., 2009). Intriguingly the invertebrate cation dop-LGIC shares close sequence homology with the vertebrate α9α10 nicotinic acetylcholine receptor (nAChR), including within the classic ligand binding domains. A great deal of previous research, including more recent structural studies have revealed residues that contribute to the binding of cholinergic ligands for nAChRs (Dani, 2015; Morales-Perez et al., 2016; Su et al., 2025); however, we found that many of these are conserved in cationic dop-LGICs (Figure 1C). In this study we sought to unravel the contribution of putative ligand binding domains and individual residues in the homomeric *Daphnia magna* dop-LGIC, Dm-DopC1, in the sensitivity of cationic dop-LGICs to catecholamines rather than cholinergic ligands like its close relatives the nAChRs.

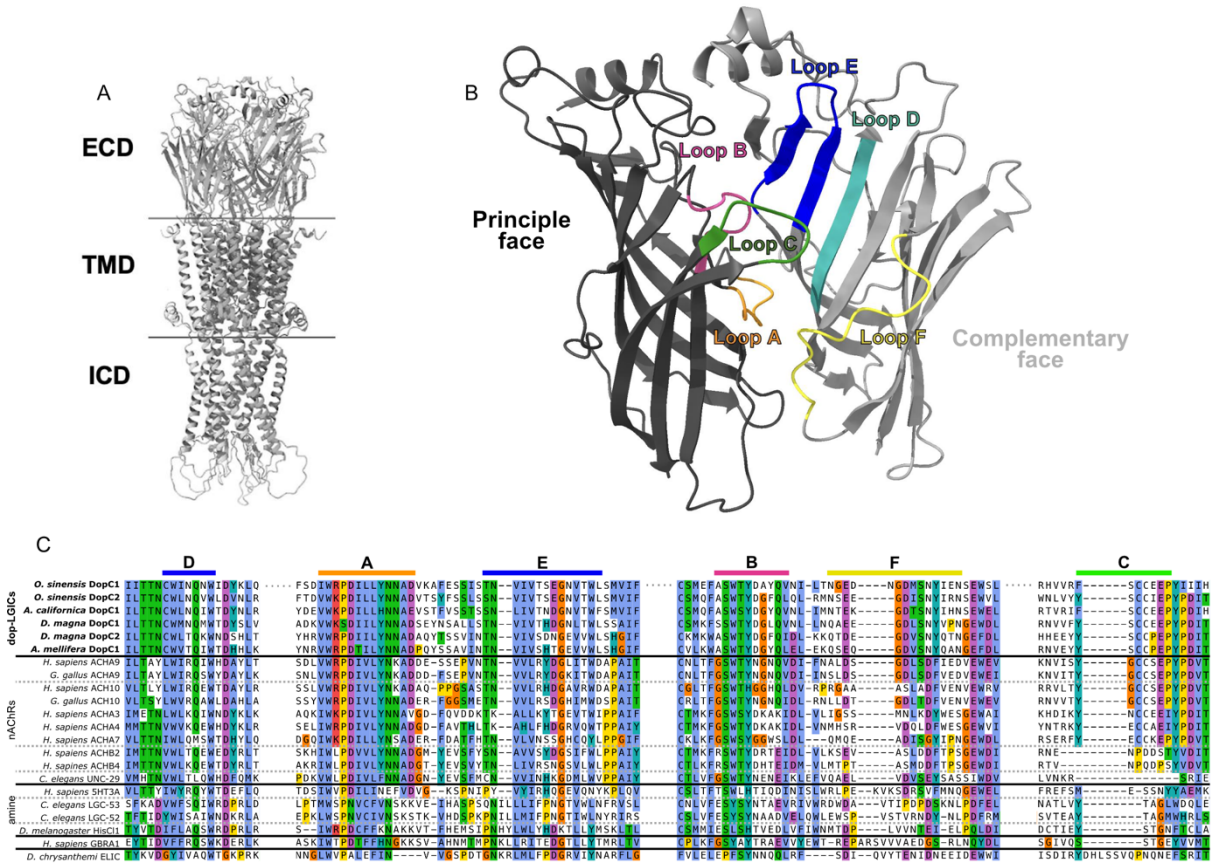

Figure 1 A. Full length AlphaFold2 model of Dm-DopC1 with the extracellular (ECD), transmembrane (TM) and intracellular (ICD) domains highlighted. **B.** Close up of the ECD and ligand binding domain made up of the interface between two adjacent subunits (light and dark grey). Extracellular loops associated with ligand binding are labeled as follows; loop A (orange), loop B (pink), loop C (green), loop D (turquoise), loop E (blue), loop F (yellow). **C.** Trimmed alignment of the ECD of dop-LGICs, nAChRs and other pLGICs showing the ligand binding loops. Alignment generated with MAFFT and residues colored with CLUSTAL coloring.

2. Materials and methods

2.1 Structural Modelling and Sequence Alignments

Amino acid sequences of a range of pLGICs (full sequences are provided in Table S 1) were aligned using the MAFTT algorithm and visualized with SnapGene (Dotmatics). Structural models were predicted using AlphaFold ColabFold. For *D. magna* Dm-DopC1, five predicted models were generated and overlaid in PyMOL. Residue positions were evaluated for consistency and model confidence (pLDDT > 70). Sites exhibiting conserved structural placement and high-confidence predictions were considered for site-directed mutagenesis.

2.2 Molecular Biology and Mutagenesis

Mutations were introduced using the Q5® Site-Directed Mutagenesis Kit (New England Biolabs). Constructs were linearized using NotI. cRNA was synthesized using the T3 mMessage mMachine Kit (ThermoFisher) and purified with the GeneJET RNA Cleanup Kit (ThermoFisher Scientific).

2.3 *Xenopus laevis* Oocyte Preparation and RNA Injection

Stage V-VI defolliculated *Xenopus laevis* oocytes were obtained from EcoCyte Bioscience and incubated in ND96 solution (in mM): 96 NaCl, 2 KCl, 1.8 CaCl2, 1 MgCl2, 5 HEPES, pH 7.5. Oocytes were stored at 18°C and injected within two days of delivery. For RNA injection, oocytes were placed in 96-well plates and injected using the Roboinject system (Multi Channel Systems, Germany). Each oocyte was injected with 50 nL of cRNA (250ng/µL). Oocytes were incubated at 18°C for 1 day prior to electrophysiological recordings.

2.4 Two-Electrode Voltage Clamp (TEVC) Recordings

TEVC recordings were performed using the Robocyte2 automated platform (Multi Channel Systems, Germany). Microelectrodes (0.5-1.5 MΩ resistance) were pulled using a P-97 micropipette puller (Sutter Instrument) and filled with 1 M KCl and 1.5 M acetic acid. Oocytes were voltage-clamped at -60 mV and recordings were sampled at 500 Hz throughout. Agonist solutions (dopamine, norepinephrine, epinephrine, tyramine, acetylcholine and serotonin) were prepared in ND96 on the day of recording and applied at concentrations ranging from 0.1 µM to 10 mM. Each ligand was perfused for 10 s followed by a 60 s wash. Wild-type oocytes were included in every recording batch. For antagonist experiment, compound solutions (50 nM to 500 µM, unless otherwise stated) were prepared in ND96 on the day of recording with 50 µM dopamine (Dm-DopC1). Before and after compound application, response to dopamine-only was recorded to obtain an Imax value per oocyte and to screen for potential irreversible binding of the antagonist. All compounds were perfused for 7 s followed by a 60 s wash. Perfusion speed was set to 3 ml/min throughout. Compounds used as antagonists: Acetylcholine chloride (Sigma-Aldrich (A6625)), Apomorphine hydrochloride (Abcam (ab269887)), Atropine (Abcam (ab145582)), Isoprenaline hydrochloride (Sigma-Aldrich (I5627)), Levamisole hydrochloride (MedChemExpress (HY-13666)), (-)-Nicotine detartrate (Abcam (ab120562)), Propranolol hydrochloride (Santa-Cruz Biotechnology (sc-3580)), (+)-Tubocurarine chloride pentahydrate (Sigma-Aldrich (93750)).

2.5 Data Analysis

All current amplitudes were exported using the Roboocyte2+ software (Multi Channel Systems) and normalized per oocyte to the maximum response (I/Imax) to account for

137 variation in expression levels using a custom python script adapted from (Morud et al., 2021).
138 Outliers were identified for each construct and removed within GraphPad Prism 10 using the
139 ROUT method (Q=1%) for every individual agonist/antagonist concentration. Agonist and
140 antagonist dose response curves were fitted in GraphPad Prism 10 using a three-parameter
141 logistic equation with a fixed Hill Slope of 1, unless otherwise stated. EC_{50} and IC_{50} values
142 were calculated from the fitted curves and reported as mean ± standard error of mean (SEM).
143 Statistical significance between wild-type and mutant dose-response curves was assessed
144 using a sum-of-squares F test. Peak current values were extracted using an existing Python
145 script (Morud et al., 2021). Normalized peak currents from the panel of ligands (1mM each:
146 tyramine, acetylcholine, norepinephrine, serotonin and epinephrine) were analyzed using a
147 one-way ANOVA followed by a Fisher's Least Significant Difference (LSD) post hoc test. All
148 TEVC recordings were baseline-subtracted unless otherwise stated. The same pooled wild-
149 type data was used for all comparisons.

150 **2.6 Software and Code Availability**

151 TEVC data were analyzed using custom Python scripts (https://github.com/hiris25/TEVC-
152 analysis-scripts). GraphPad Prism 10 was used for data plotting and fitting. MAFFT (Katoh
153 and Standley, 2013) was used for sequence alignment, alignments were visualized in
154 snapgene and ChimeraX 1.9 was used for 3D structural visualization. All constructs and raw
155 data are available upon request.

156

157 **3. Results**

158 **3.1 Despite strong conservation with nAChRs, residues in loop C contribute to**
159 **catecholamine sensitivity and selectivity**

160 The principle or α-type subunit contributes three structurally distinct loops to the ligand
161 binding domain, with loop C forming the front outer side of the binding pocket that closes
162 around the ligand during receptor activation and loops A and B forming the back of the
163 binding pocket (Dani, 2015; Morales-Perez et al., 2016). Loop C contains two conserved
164 structural features in nAChRs. The first is a pair of tyrosines implicated in aromatic cage
165 formation (Braun et al., 2016; Celie et al., 2004; Tomaselli et al., 1991) and the second is a
166 double cystine motif (Tomizawa et al., 2008) together forming a 'YXCC' motif. Both features
167 are present in dop-LGICs and in Dm-DopC1 are represented by Y226 and Y233, and the
168 C228 - C229, respectively (Figure 2E-F). Notably though both human and chicken nAChR
169 α9 and α10 subunits contain a glycine at the 'X' position, while the dop-LGICs contain serine
170 at this position. When we substituted S227 for glycine at this position in Dm-DopC1 we

171 observed a significant reduction in sensitivity to all catecholamines (Figure 2A-C). The
172 largest shift was seen with dopamine, shifting 7-fold from a WT EC_{50} of 84μM to 589μM,
173 norepinephrine EC_{50} also shifted 4-fold and epinephrine 1.8-fold (Figure 2A-C). This
174 suggests that the native serine may stabilise local interactions required for maintaining the C
175 loop conformation or supporting neighbouring aromatic residues for catecholamine
176 recognition.

177 We were also interested in the residue immediately following the 'YXCC' motif, which is
178 divergent across species and receptor types. However, both Dm-DopC2 and Am-DopC1
179 (from *Apis mellifera*), which have a higher relative selectivity for dopamine vs. the other
180 catecholamines, encode a proline at this position. A substitution to proline in this position in
181 Dm-DopC1 (E230P) produced a selective decrease in norepinephrine sensitivity only, with a
182 4-fold shift of EC_{50} from 98μM to 401μM, while maintaining wild type sensitivity for dopamine
183 and epinephrine (Figure 2A-C). However, despite altering the relative sensitivities, the
184 E230P mutation did not alter the ligand binding profile of the receptor, with norepinephrine
185 still eliciting similar relative peak currents to dopamine and epinephrine at 1mM (Figure 2D).
186 In contrast S227G which altered sensitivity to all catecholamines, abelite with more
187 pronounced shift in dopamine sensitivity, did alter the ligand binding profile such that
188 dopamine induced currents at 1mM fell significantly to approximately 50% of the maximum
189 currents achieved with norepinephrine and epinephrine (Figure 2D). Together these data
190 suggest that despite key nAChR features of loop C being conserved between cholinergic
191 and catecholamine binding receptors, the surrounding residues also contribute to ligand
192 specificity and binding capability.

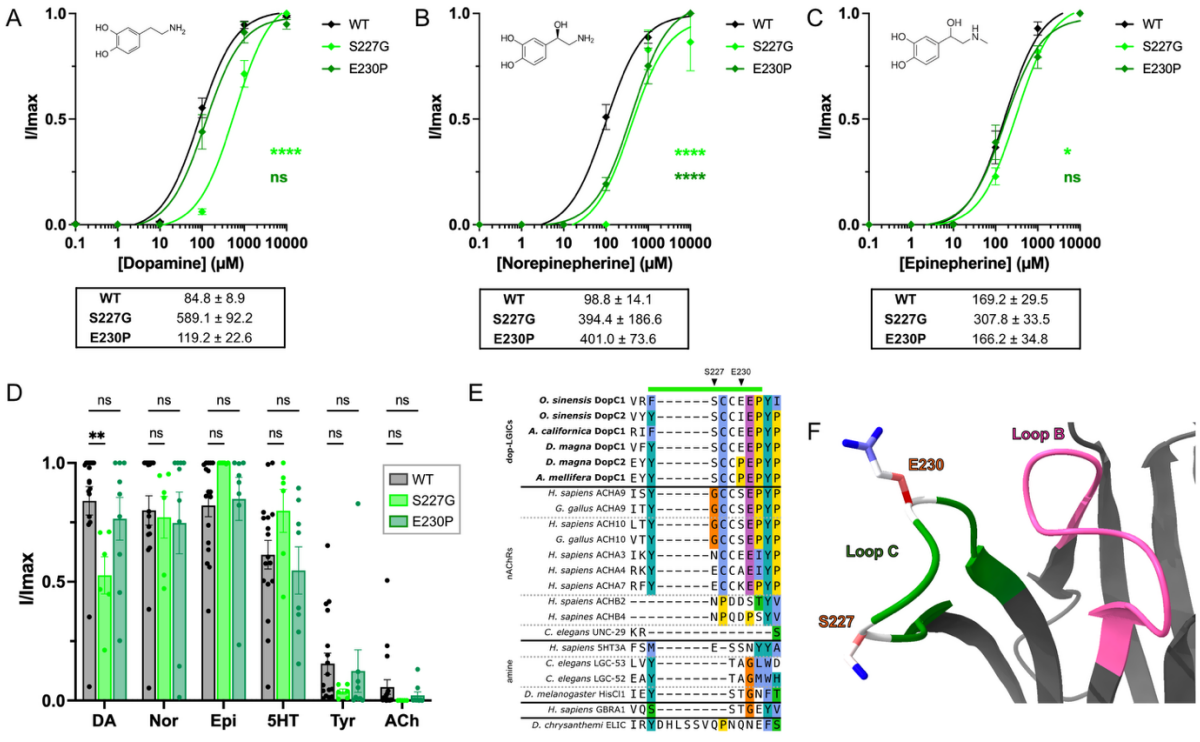

Figure 2 Mutations in Loop C of a *D. magna* dop-LGIC reduce catecholamine sensitivity and alter agonist selectivity. A-C. Dose response curves for dopamine (A), norepinephrine (B) and epinephrine (C) in wild-type, S227G and E230P Dm-DopC1 expressing *Xenopus* oocytes. Current normalized by I/Imax. EC_{50} values (± SEM) shown below each plot. **** = P<0.0001, * = P<0.05, ns = not significant calculated by sum of squares F test. WT: *n* = 24 (dopamine), 12 (norepinephrine), 11 (epinephrine); S227G: *n* = 6 (dopamine), 3 (norepinephrine), 5 (epinephrine); E230P: *n* = 10 (dopamine), 4 (norepinephrine), 9 (epinephrine). **D.** Relative maximum I/Imax currents of *Xenopus* oocytes expressing wild-type, S227G and E230P Dm-DopC1, perfused for 10 s with 1 mM each: dopamine (DA), norepinephrine (Nor), epinephrine (Epi), serotonin (5HT), tyramine (Tyr), and acetylcholine (ACh). WT: *n* = 18 (dopamine, norepinephrine, ACh, tyramine), 17 (epinephrine, serotonin); S227G: *n* = 11 per agonist; E230P: *n* = 6 per agonist. ** = P<0.01, ns = not significant by one-way ANOVA and a Fisher's LSD. **E.** Sequence alignment of the Loop C region. Residues S227 and E230 indicated by arrows, loop C is highlighted by the green bar. **F.** AlphaFold2 model of the loop C (green) region of Dm-DopC1 with S227 and E230 relative to Loop B (pink) at the ligand-binding site.

3.2 A conserved aspartate in loop B of principle face is critical to catecholamine sensitivity

Loop B forms part of the back wall of the ligand binding domains on the principle face and contains one of the conserved tryptophans forming the aromatic cage which is part of a

214 conserved region encoded the consensus motif ‘SWTY’ (Figure 3E-F). A semi conserved
215 glycine, 4 amino acids downstream of the tryptophan has been implicated in defining high
216 and low potency nAChRs (Puskar et al., 2012). In the dop-LGICs this post-tryptophan
217 glycine is broadly conserved and directly preceded by an aspartate which is conserved
218 across the dop-LGICs but not found in vertebrate α9/10 receptors. Substitution of this
219 position (D188) in Dm-DopC1 with asparagine, more commonly found in nAChRs, led to a
220 striking reduction in catecholamine sensitivity, leading to EC_{50} values for all three ligands of
221 over 9mM, although true EC_{50} values could not be calculated due to lack of saturation even
222 at 10mM (Figure 3A-C). The D188N mutation also led to significant changes in ligand
223 binding profiles at 1mM with norepinephrine currents significantly reduced to 8% of the
224 maximal currents, dopamine reduced to 37% and serotonin induced currents also falling to
225 19% (Figure 3D). However, it is worth noting that there was no appreciable difference in
226 acetylcholine currents, which along with the residual currents observed from the
227 catecholamines suggests that while loop B is critical to catecholamine gating, this single
228 residue switch is insufficient in defining catecholamine vs cholinergic activation.

229 We also noted an additional residue of interest downstream of loop B, which differed only in
230 Dm-DopC1 compared to other dop-LGICs and vertebrate α9/10. Given the differences in
231 selectivity between Dm-DopC1 and Dm-DopC2 we hypothesised that the conserved
232 aspartate at this position may also be contributing to ligand selectivity. Mutation at this
233 location in Dm-DopC1 (N193D), led to a significant increase in EC_{50} for all catecholamines,
234 most notably for norepinephrine with a 11-fold shift resulting in an EC_{50} of 1087μM, with
235 smaller yet statistically significant shifts for dopamine and epinephrine of approximately 2-
236 fold (Figure 3A-C). There was no change in overall ligand binding profile with all 3
237 catecholamines still eliciting the largest currents (Figure 3D). This suggests that the
238 conserved aspartate at this position may contribute to selectivity between catecholamines,
239 with receptors bearing this residue being relatively more selective for dopamine.

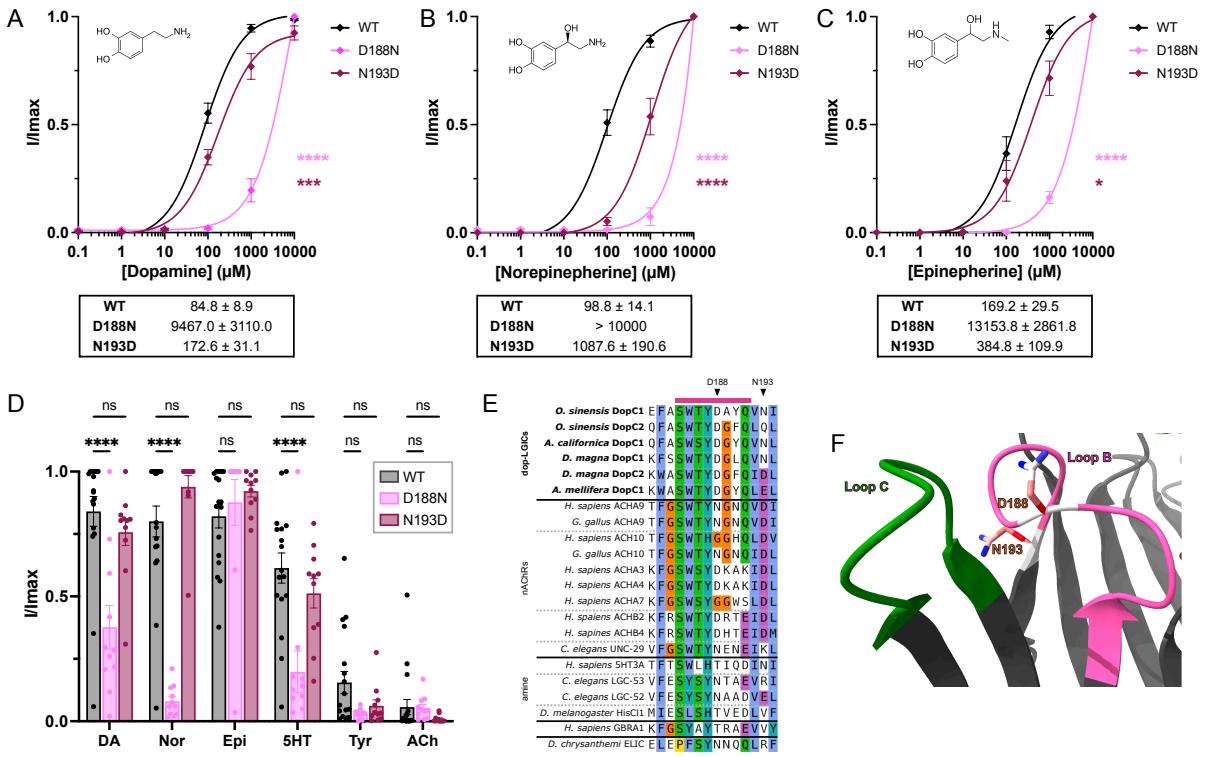

Figure 3 Mutations in Loop B of Dm-DopC1 disrupt catecholamine sensitivity and alter ligand selectivity. A-C. Dose response curves for dopamine (A), norepinephrine (B) and epinephrine (C) in wild-type, D188N and N193D Dm-DopC1 expressing *Xenopus* oocytes. Current normalized by I/Imax. EC_{50} values (± SEM) shown below each plot. **** = P<0.0001, *** = P<0.001, * = P<0.05 calculated by sum of squares F test. WT: *n* = 24 (dopamine), 12 (norepinephrine), 11 (epinephrine); D188N: *n* = 10 (dopamine), 5 (norepinephrine), 9 (epinephrine); N193D: *n* = 15 (dopamine), 5 (norepinephrine), 7 (epinephrine). **D.** Relative maximum I/Imax currents of *Xenopus* oocytes expressing wild-type, D188N and N193D Dm-DopC1, perfused for 10 s with 1 mM each: dopamine (DA), norepinephrine (Nor), epinephrine (Epi), serotonin (5HT), tyramine (Tyr), and acetylcholine (ACh). WT: *n* = 18 (dopamine, norepinephrine, ACh, tyramine), 17 (epinephrine, serotonin); D188N: *n* = 11 per agonist; N193D: *n* = 11 per agonist. **** = P<0.0001, ns = not significant by one-way ANOVA and a Fisher's LSD. **E.** Sequence alignment of the Loop B region. Residues D188 and N193 indicated by arrows, loop B is highlighted by the pink bar. **F.** AlphaFold2 model of the loop B (pink) region of Dm-DopC1 with D188N and N193D relative to Loop C (green) at the ligand-binding site.

3.3 Residues on the complementary face of the binding pocket contribute to dopamine sensitivity and selectivity

In addition to the principal subunit, two loops on the complementary face of the binding pocket have also been shown to be involved in ligand binding in nAChRs. Loop D is composed of a single β strand and forms the base of the binding site, while loop E is

262 composed of two β strands connected by a short loop. We observed that loop D was broadly
263 conserved between both nAChRs and dop-LGICs, however we again noted that the two
264 dop-LGICs with higher dopamine selectivity, Dm-DopC2 and Am-DopC1, encoded a
265 threonine in the centre of the loop (Figure 4E-F). Creating this change in Dm-DopC1, N92T,
266 led to a striking and significant reduction of norepinephrine sensitivity, with an EC_{50} increase
267 from 98μM to 439μM, with no effect on dopamine or epinephrine (Figure 4A-C) and no
268 changes to overall ligand binding profile at 1mM (Figure 4D).This suggests that the threonine
269 at this position is important for discerning between norepinephrine and the other
270 catecholamines.

271 Despite overall high similarity within loop E, sequence alignments revealed a strongly
272 conserved aspartate at the proximal end of loop E in α9/10 that is missing from the dop-
273 LGICs, which frequently encode a hydrophobic leucine or phenylalanine at this position
274 (Figure 4E-F). When we substituted leucine with aspartate at this location in Dm-DopC1 we
275 could not generate functional receptors that responded to any of the ligands tested, although
276 due to leak current in oocytes we hypothesise that the protein was expressed (Figure S 1G).
277 This suggests that leucine at this position is critical to either channel formation or ligand
278 binding. Additionally, we also noted that the two more-dopamine selective dop-LGICs, Dm-
279 DopC2 and Am-DopC1, had a substitution of an alanine conserved across both receptor
280 types with a glycine (Figure S 1E-F). Despite being a minor alteration in sequence we found
281 that this substitution in Dm-DopC1, A158G, led to small but significant increases in EC_{50} for
282 all catecholamines to similar extents (EC_{50}s: dopamine: 235μM, norepinephrine: 440μM,
283 epinephrine: 438μM) (Figure S 1A-D). Again, supporting the notion that residues
284 surrounding key ligand binding loops contribute to receptor function, likely through the
285 stabilisation of these regions.

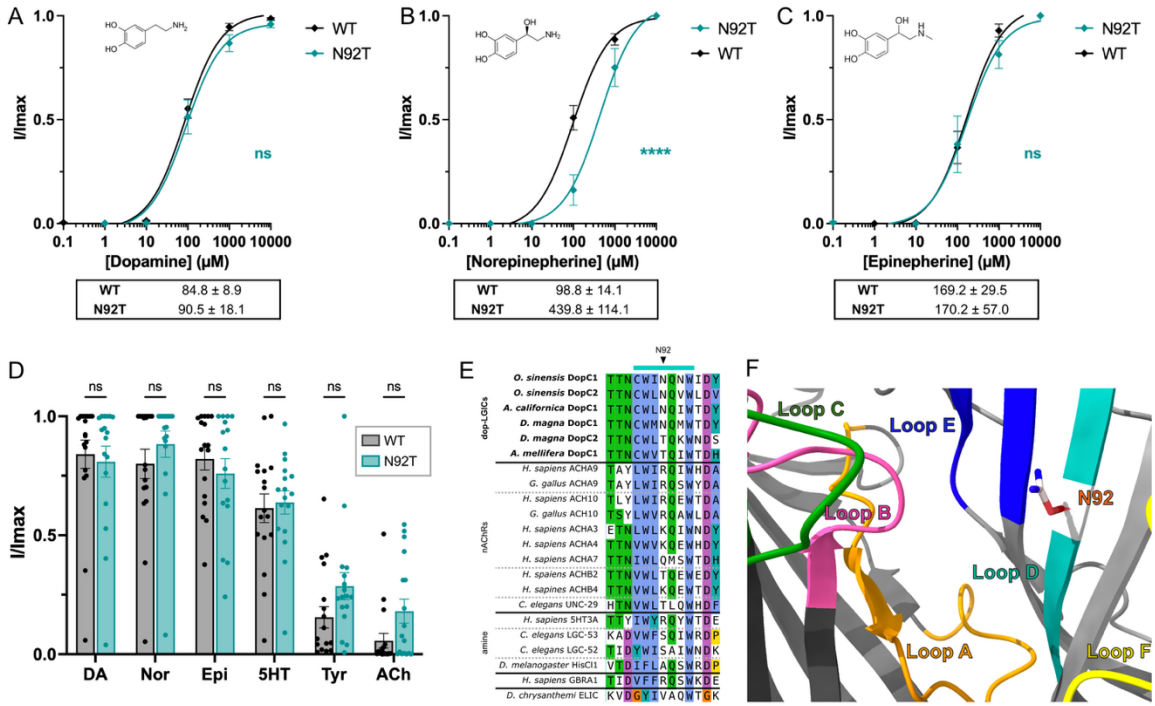

Figure 4 The N92T mutation in Loop D of a *D. magna* dop-LGIC reduces norepinephrine sensitivity but preserves agonist selectivity. A-C. Dose response curves for dopamine (A), norepinephrine (B) and epinephrine (C) in wild-type and N92T Dm-DopC1 expressing *Xenopus* oocytes. Current normalized by I/Imax. EC_{50} values (± SEM) shown below each plot. **** = P<0.0001, ns = not significant calculated by sum of squares F test. WT: *n* = 24 (dopamine), 12 (norepinephrine), 11 (epinephrine); N92T: *n* = 10 (dopamine), 5 (norepinephrine), 8 (epinephrine). **D.** Relative maximum I/Imax currents of *Xenopus* oocytes expressing wild-type and N92T Dm-DopC1, perfused for 10 s with 1 mM each: dopamine (DA), norepinephrine (Nor), epinephrine (Epi), serotonin (5HT), tyramine (Tyr), and acetylcholine (ACh). WT: *n* = 18 (dopamine, norepinephrine, ACh, tyramine), 17 (epinephrine, serotonin); N92T: *n* = 11 per agonist. ns = not significant by one-way ANOVA and a Fisher's LSD. **E.** Sequence alignment of the loop D region. Residue N92 is indicated by an arrow, loop D is highlighted by the turquoise bar. **F.** AlphaFold2 model of the loop D (turquoise) region of Dm-DopC1 with N92 relative to loop B (pink), loop C (green), loop F (yellow), loop A (orange) and loop E (blue) at the ligand-binding site.

3.4 The conserved proline of loop A enhances catecholamine sensitivity

In line with previous findings, our sequence alignments identified a proline residue conserved across all pLGICs that sits within the conserved 'WXPD' motif (Figure 5E-F) (Braun et al., 2016). However, in Dm-DopC1 this location encodes a serine, which AlphaFold2 structural modelling placed near the inter-subunit ligand-binding interface, in proximity to Loops B and C (Figure 5F). Strikingly, restoring the proline at this position in Dm-DopC1 (S123P)

significantly increased sensitivity to all catecholamines (Figure 5A-C). Dopamine EC_{50} decreased from 84.82 ± 9.1 µM to 39.84 ± 6.06 µM, norepinephrine from 98.78 ± 14.09 µM to 36.52 ± 7.86 µM, and epinephrine from 169.17 ± 29.5 µM to 47.87 ± 14.05 µM (Figure 5A-C). Interestingly, unlike the other mutations examined in this study, S123P also led to an increase in Hill slope for norepinephrine (2.16 ± 0.19) compared to WT (1.31 ± 0.30), suggesting enhanced co-operativity (Figure S 2). Overall, the relative ligand binding profile was unaltered, although there was a small but non-significant increase in relative acetylcholine current (Figure 5D).

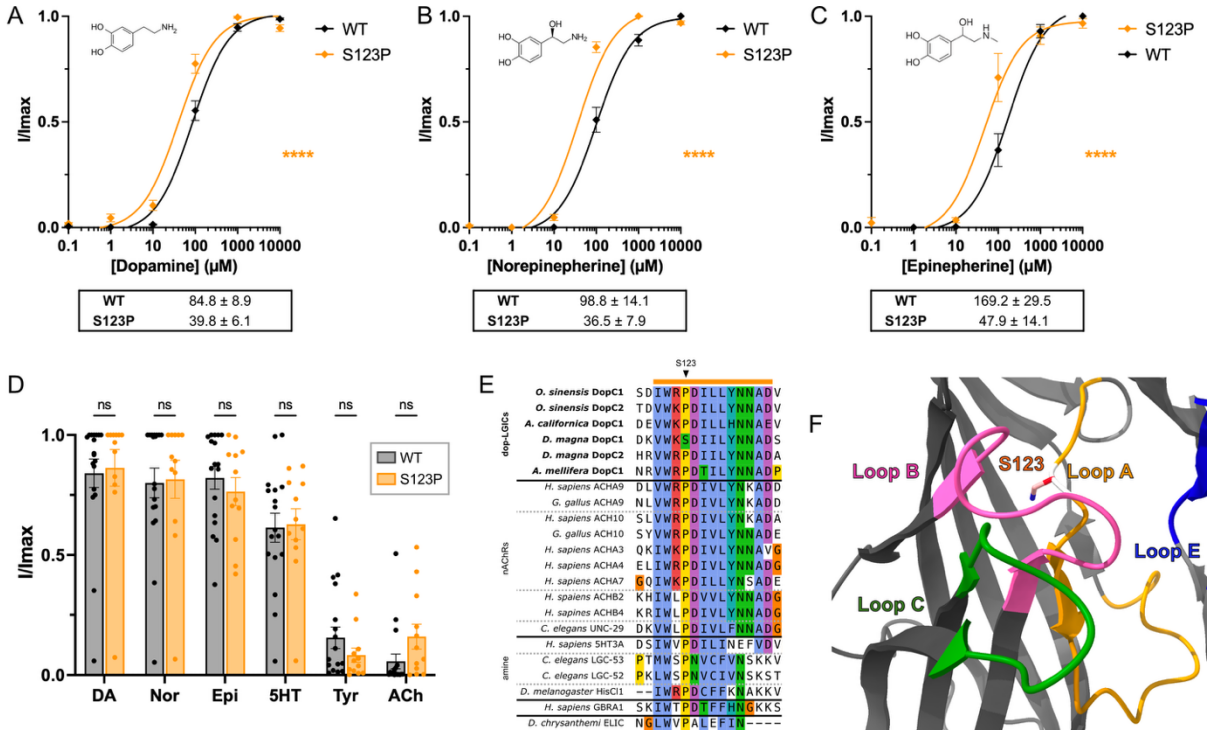

Figure 5 The conserved proline of loop A is required for ligand sensitivity in dop-LGICs. A-C. Dose response curves for dopamine (A), norepinephrine (B) and epinephrine (C) in wild-type and S123P Dm-DopC1 expressing *Xenopus* oocytes. Current normalized by I/Imax. EC_{50} values (± SEM) shown below each plot. **** = P<0.0001 calculated by sum of squares F test. WT: *n* = 24 (dopamine), 12 (norepinephrine), 11 (epinephrine); S123P: n = 12, (dopamine), 4 (norepinephrine) and 8 (epinephrine). **D.** Relative maximum I/Imax currents of *Xenopus* oocytes expressing wild-type and A158G Dm-DopC1, perfused for 10 s with 1 mM each: dopamine (DA), norepinephrine (Nor), epinephrine (Epi), serotonin (5HT), tyramine (Tyr), and acetylcholine (ACh). WT: *n* = 18 (dopamine, norepinephrine, ACh, tyramine), 17 (epinephrine, serotonin); S123P: n = 12 per agonist. ns = not significant by one-way ANOVA and a Fisher's LSD. **E.** Sequence alignment of the loop E region. Residue S123 is indicated by an arrow, loop A is highlighted by the orange bar. **F.** AlphaFold2 model of the loop A (orange) region of

329 Dm-DopC1 with S123 relative to loop B (pink), loop C (green) and loop E (blue) at the ligand-
330 binding site.

331 **3.5 Cholinergic, dopaminergic and adrenergic compounds antagonise dop-LGICs**

332 To further dissect the pharmacology of the cationic dop-LGICs we tested a range of
333 cholinergic, dopaminergic and adrenergic compounds for their ability to activate or
334 antagonise Dm-DopC1. We found that both Dm-DopC1 dopamine induced currents could be
335 blocked by the nicotinic antagonist tubocurarine, with an IC_{50} of 0.9μM (Figure 6A). In
336 contrast to other nAChRs, the vertebrate a9/10 nAChRs are antagonised by nicotine
337 (Elgoyhen et al., 2001, 1994). In line with this we found that the dopamine currents of Dm-
338 DopC1 could be blocked at high concentrations of nicotine with and IC_{50} of 109μM (Figure
339 6A). We also tested the muscarinic blocker, atropine, which has been shown to act on
340 nAChRs (Parker et al., 2003; Zwart and Vijverberg, 1997), for its ability to block dopamine
341 currents and found that it behaved similarly to nicotine with relatively poor blocking (IC_{50}:
342 101μM (Figure 6A). This family of dop-LGICs have also been shown to be minimally
343 activated by acetylcholine (Courtney et al., 2025), and due to their close homology with
344 nAChRs and antagonism by nicotine we sought to determine if acetylcholine is able to
345 interact with the dopamine induced current, however we saw no evidence of this (Figure 6A).
346 In addition, we also tested apomorphine, a non-selective vertebrate dopamine receptor
347 agonist and the β-adrenoceptor agonist and antagonist, isoprenaline and propranolol
348 respectively. Apomorphine was able to block the dopamine induced current of Dm-DopC1,
349 with an IC_{50} of 6μM (Figure 6B). Meanwhile propranolol but not isoprenaline was able to
350 block dopamine currents (IC_{50}: 100μM) (Figure 6B). We also tested the ability of these
351 compounds to activate the receptors and observed no activation at 100μM (Figure S 3).

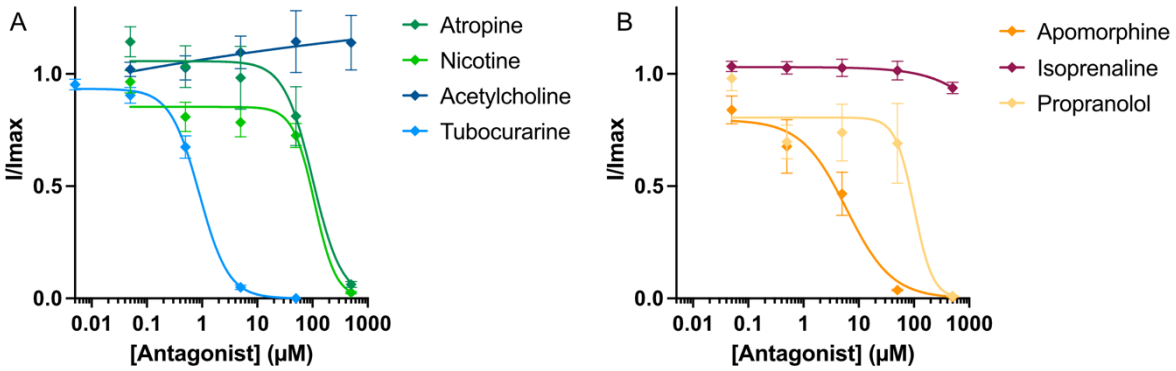

Atropine	101.3 ± 37.3
Nicotine	108.8 ± 40.0
Acetylcholine	nd
Tubocurarine	0.9 ± 0.1

Apomorphine	6.0 ± 2.4
Propranolol	100.5 ± 108.0
Isoprenaline	nd

352

353 **Figure 6 Dm-DopC1is sensitive to antagonism by cholinergic and dopaminergic**
354 **compounds**. **A-B.** Inhibitory dose response curves for a panel of cholinergic (A) and
355 dopaminergic and adrenergic compounds (B). Error bars represent SEM. *n* = 4
356 (apomorphine, isoprenaline), 6 (atropine, propranolol), 9 (tubocurarine, acetylcholine), 12
357 (nicotine). IC50s are shown below each plot and calculated with a 4-parameter curve with
358 constrained bottom = 0, nd = not determined.

359

360 ## 4. Discussion

361 Despite high levels of conservation of key ligand binding motifs with vertebrate and
362 invertebrate nAChRs this new class of dopamine-gated cation channels displays striking
363 differences in ligand sensitivity and antagonism by a range of compounds. In this study we
364 highlight some of the key residues that likely contribute to this functional difference (Table 1),
365 with many surrounding previously defined key motifs for cholinergic receptors.

366 Table 1 **Summary of Ec50 values for all tested mutations.** All values are given in μM and
367 calculated using a 3-parameter curve fit with a Hill slope of 1. P values were calculated using
368 the sum of squares F test.

		Dopamine			**Norepinephrine**			**Epinephrine**		
		E_C50	SEM	P value	E_C50	SEM	P value	E_C50	SEM	P value
Loop	**Construct**									
	WT	84.8	8.9	N/A	98.8	14.1	N/A	169.2	29.5	N/A
A	S123P	39.8	6.1	<0.0001	36.5	7.9	<0.0001	47.9	14.05	<0.0001
B	D188N	9466.9	3110	<0.0001	Unstable	Unstable	<0.0001	13153.8	2861.8	<0.0001
	N193D	172.6	31.1	0.0003	1087.9	190.6	<0.0001	384.8	109.9	0.0163
C	S227G	589.1	92.2	<0.0001	394.4	186.6	<0.0001	307.8	33.5	0.0262

	E230P	119.2	22.6	0.0812	401.1	73.6	<0.0001	166.2	34.8	0.9494
D	N92T	90.5	18.1	0.7445	439.8	114.1	<0.0001	170.2	57	0.9868
E	L155D	-	-	-	-	-	-	-	-	-
	A158G	234.6	30.7	<0.0001	439.8	57.5	<0.0001	438.2	57.97	<0.0001

The most striking effect was the almost complete loss of catecholamine gating upon replacement of an aspartate in loop B (D188N) which follows the conserved 'SWTY' motif and which is conserved in dop-LGICs. To our knowledge, this site, which in vertebrate α9/10 encodes an asparagine or glycine, has not been previously directly implicated in ligand binding for nAChRs. However, it is unlikely that this residue alone contributes to dopamine selectivity over cholinergic ligands given that aspartate is also found at this position in classic nAChRs such as human α4 and the lack of significant acetylcholine gating over the wild type for this mutation in Dm-DopC1. Interestingly, though immediately following this aspartate is a semi conserved glycine residue which has been shown to distinguish high affinity vertebrate nAChRs (eg. α4 which encodes lysine at this position) from low affinity receptors (eg. α7 which encodes glycine). The increased affinity is thought to be due to stabilization of the open and desensitized states by virtue of a hydrogen bond between this position in loop B and a proline in loop C that forms in absence of glycine (Grutter et al., 2003; Kouvatsos et al., 2016; Puskar et al., 2012). Interestingly glycine is present at this position in all but one dop-LGIC (which instead encodes an alanine) further supporting the hypothesis that this hydrogen bond is key to high affinity acetylcholine receptors. Decoupling of loops B and C may be important for gating by aminergic ligands given that monoamine gated receptors from other subfamilies such as the vertebrate $5HT_3R$ and invertebrate chloride permeable dopamine and histamine receptors lack the hydrogen forming proline within loop C. In addition, loop B also contains one of the conserved tryptophans associated with aromatic cage formation. Preceding this tryptophan by 2 amino acids is another glycine residue conserved in nAChRs α subunits but encoding an arginine in β subunits, which causes movements in the tryptophan preventing it from forming a functional binding site (Morales-Perez et al., 2016), in dop-LGICs this site encodes a alanine or serine. Mutations in loop B have also been shown to be more broadly required for monoamine binding in $5HT_3Rs$ for example (Thompson et al., 2008). It would be interesting to see if the D188N reverse mutation in vertebrate receptors alters acetylcholine gating, although given the divergence of sequences at this position across nAChRs in both

397 vertebrates and invertebrates this residue may not be contributing in a significant way to
398 acetylcholine recognition.

399 We also confirmed the importance, yet surprising flexibility, of a highly conserved proline
400 residue within the 'WXPD' motif of loop A, which has been hypothesized to be critical for
401 maintaining structural integrity and receptor assembly in pLGIC receptors from bacteria
402 through to humans (Braun et al., 2016). We observed that Dm-DopC1, which exhibits a higher
403 EC_{50} for dopamine than other dop-LGICs (Courtney et al., 2025), diverged from this motif to
404 encode serine at this position (WKSD), which when substituted for proline, led to significant
405 increases in catecholamine sensitivity. The mirrors previous work in glycine receptors where
406 the same proline was replaced by an alanine leading to a decrease in ligand sensitivity
407 (Hughes et al., 2020; Lummis and Dougherty, 2022). Not only does our finding further highlight
408 the importance of a proline at this position, but it also shows that there is flexibility in the motif,
409 as the natural variant still displays micromolar ligand binding. As this serine is not conserved
410 within the rest of the dop-LGIC group, it is unlikely to be directly participating in catecholamine
411 recognition. Rather this suggests, as has been previously hypothesized, that the conserved
412 proline of the 'WXPD' motif contributes indirectly by stabilizing loop A conformation or
413 facilitating ligand alignment within the binding pocket.

414 An intriguing feature of the invertebrate cationic dop-LGICs is the presence of key motifs
415 usually attributed to acetylcholine and nicotine binding in nAChRs. This is highlighted by loop
416 C, which in dop-LGICs also encodes the conserved 'YXCC' motif (Karlin, 2002; Tomizawa et
417 al., 2008) as well as a pair of tyrosines implicated in aromatic cage formation (Braun et al.,
418 2016). However, the at 'X' position of the 'YXCC' motif the dop-LGICs encode a conserved
419 serine, which is not present in nAChRs. By exchanging this serine for glycine (present in
420 α9/10) in Dm-DopC1, we found that this serine is indeed important for catecholamine gating
421 but did not confer acetylcholine gating despite restoring the motif often found in nAChRs.
422 Separately, we also found that the residue immediately downstream of the 'YXCC' motif was
423 important for determining differences in ligand sensitivity between *Daphnia* dop-LGICs. The
424 functional impact of mutations at these positions supports the established role of loop C in
425 maintaining the geometry of the ligand binding pocket, particularly in orienting conserved
426 aromatic residues that contribute to catecholamine recognition. It also echoes our findings
427 within loop B, which suggests that a series of changes in the binding regions are required to
428 completely alter receptor selectivity from cholinergic to dopaminergic.

429 We also explored the role of loops D, E and F that form the complimentary face of the ligand
430 binding pocket and have been shown to contribute to stabilizing the extracellular domain. A
431 key feature of Loop D is the 'WXD' motif that is conserved across nAChRs, dop-LGICs,

432 5HT$_3$Rs and even some chloride channels (Braun et al., 2016; Corringer et al., 1995; Spier
433 and Lummis, 2000). Loop D is remarkably well conserved between dop-LGICs and nAChRs,
434 suggesting that its main function is to stabilize the ligand binding regions. However, we did
435 note that both Dm-DopC2 and Am-DopC1, which are more selective for dopamine than the
436 other dop-LGICs encoded a threonine 2 amino acids before the 'WXD' motif, rather than an
437 asparagine. When we substituted this asparagine for threonine in Dm-DopC1 we noted a
438 specific alteration in ligand sensitivity with only the norepinephrine EC_{50} being adversely
439 affected while dopamine and epinephrine responses remained like wild type, making the
440 receptor overall more selective for dopamine. Interestingly, vertebrate nAChRs typically
441 encode a lysine or arginine at this position which is also conserved across other pLGICs
442 including glycine and GABA receptors, where disruption of this residue leads to almost
443 complete loss of ligand activation (Goldschen-Ohm et al., 2011; Grudzinska et al., 2005). The
444 cationic dop-LGICs, in line with hypotheses drawn up by Lynagh and Pless in 2014, also lack
445 positively charged residues in this position instead favoring polar residues also found in other
446 amine gated receptors including HisCl and the anionic dop-LGICs from nematodes, which
447 may assist in binding the hydroxyl termini or these ligands (Lynagh and Pless, 2014).
448 Collectively these mutations have identified residues critical for catecholamine recognition
449 across various conserved ligand binding domains, revealing that like in other pLGICs, both
450 faces of the ligand binding domain are critical not only for ligand gating but also relative ligand
451 selectivity. However, this study also demonstrates that ligand switching from acetylcholine to
452 (or from) dopamine requires a series of alterations across evolutionary time.

453 Finally, we also examined the pharmacology of dop-LGICs by testing a range of cholinergic,
454 dopaminergic and adrenergic compounds for their ability to interact with the dopamine induced
455 currents from both Dm-DopC1. The competitive nAChR antagonist, tubocurarine (Rahman et
456 al., 2022), efficiently blocked currents in the low μM range, broadly in line with classic nAChRs
457 (Zwart and Vijverberg, 1998). In contrast, other cholinergic compounds such as nicotine and
458 atropine (a muscarinic antagonist) had effects only at high concentrations. This is in line with
459 evidence that tubocurarine can act on a broader range of pLGICs including vertebrate 5HT$_3$Rs
460 (Peters et al., 1990; Yan et al., 1998) and invertebrate chloride gated cholinergic receptors
461 (Hardege et al., 2023). In addition, dop-LGICs could be blocked by apomorphine (non-
462 selective vertebrate dopamine agonist) and propranolol (β-adrenoceptor antagonist) in the μM
463 range suggesting that dop-LGICs have a distinct pharmacology from their closely related
464 nAChRs, with the potential of novel chemistries to be used to target this subfamily.

465 **5. Conclusion**

In this study we detail the mechanistic map of ligand selectivity of the invertebrate dopamine-gated cation channel (dop-LGIC) family, extending the known functional repertoire of these receptors. Our primary aim was to identify how variations in conserved ligand binding domains enable dop-LGICs to respond selectively to catecholamines rather than cholinergic ligands, despite their close sequence homology with vertebrate nAChRs. In line with this we found that while core structural features of the pLGIC superfamily are conserved, functional divergence is driven by key residue variations surrounding these canonical motifs in the extracellular loops. We identified residues critical for catecholamine recognition across loops typically associated with both the principal (A-C) and complementary faces (D-F) of the ligand binding domain. Pharmacological analysis of dop-LGICs also confirmed a distinct profile from their nAChR relatives, with dopamine-induced currents efficiently blocked in the micromolar range by cholinergic, dopaminergic and adrenergic compounds.

Our results provide insight into the functional plasticity within invertebrate neurotransmission systems and reveal how subtle differences in loop composition enable the switch from cholinergic to aminergic ligand recognition. The fact that cationic dop-LGICs are conserved across multiple invertebrate species, confirms the widespread nature of this signaling mechanism. Furthermore, the demonstrated requirement for a series of evolutionary changes to achieve ligand switching raises fundamental questions about the origin of ionotropic neurotransmission, specifically whether dopamine or acetylcholine signaling emerged first. Future research should focus on comparative structural analysis of dop-LGICs across basal phyla, such as Platyhelminths or Nematodes (where unique anionic dop-LGICs are already found), to trace the evolutionary trajectory and structural requirements that drove the transition between cholinergic and dopaminergic ionotropic signaling.

Funding

I.H. and this work was kindly supported by a Royal Society University Research Fellowship (URF\R1\231648).

Acknowledgements

The authors gratefully acknowledge Howard Baylis and all present and past members of the Hardege lab for helpful discussions.

Author Contributions

T. M. M: Conceptualization, Methodology, Validation, Formal analysis, Investigation, Data Curation, Writing - Original Draft, Visualization. **T. E. R:** Methodology, Validation, Formal analysis, Investigation, Data Curation, Writing - Review & Editing. **I. H:** Conceptualization, Formal analysis, Resources, Data Curation, Writing - Original Draft, Visualization, Supervision, Project administration, Funding acquisition.

Declaration of interest

The authors declare no competing interests.

References

Boulin, T., Gielen, M., Richmond, J.E., Williams, D.C., Paoletti, P., Bessereau, J.-L., 2008. Eight genes are required for functional reconstitution of the Caenorhabditis elegans levamisole-sensitive acetylcholine receptor. Proceedings of the National Academy of Sciences 105, 18590–18595. https://doi.org/10.1073/pnas.0806933105

Braun, N., Lynagh, T., Yu, R., Biggin, P.C., Pless, S.A., 2016. Role of an Absolutely Conserved Tryptophan Pair in the Extracellular Domain of Cys-Loop Receptors. ACS Chem. Neurosci. 7, 339–348. https://doi.org/10.1021/acschemneuro.5b00298

Celie, P.H.N., van Rossum-Fikkert, S.E., van Dijk, W.J., Brejc, K., Smit, A.B., Sixma, T.K., 2004. Nicotine and carbamylcholine binding to nicotinic acetylcholine receptors as studied in AChBP crystal structures. Neuron 41, 907–914. https://doi.org/10.1016/s0896-6273(04)00115-1

Corringer, P.-J., Baaden, M., Bocquet, N., Delarue, M., Dufresne, V., Nury, H., Prevost, M., Van Renterghem, C., 2010. Atomic structure and dynamics of pentameric ligand-gated ion channels: new insight from bacterial homologues. J Physiol 588, 565–572. https://doi.org/10.1113/jphysiol.2009.183160

Corringer, P.J., Galzi, J.L., Eiselé, J.L., Bertrand, S., Changeux, J.P., Bertrand, D., 1995. Identification of a new component of the agonist binding site of the nicotinic alpha 7 homooligomeric receptor. J Biol Chem 270, 11749–11752. https://doi.org/10.1074/jbc.270.20.11749

Courtney, A., Styfhals, R., Dijck, M.V., Boulanger, J., Geenen, L., Lanoizelet, M., Hardege, I., Lassnig, M., Jansson, A.M., Gehler-Rahman, J., Almansa, E., Obenhaus, H.A., Seuntjens, E., Schafer, W.R., 2025. Novel dopaminergic neurotransmission in the Octopus visual system. https://doi.org/10.1101/2025.04.02.646353

Cully, D.F., Paress, P.S., Liu, K.K., Schaeffer, J.M., Arena, J.P., 1996. Identification of a Drosophila melanogaster glutamate-gated chloride channel sensitive to the antiparasitic agent avermectin. J Biol Chem 271, 20187–20191. https://doi.org/10.1074/jbc.271.33.20187

Cully, D.F., Vassilatis, D.K., Liu, K.K., Paress, P.S., Van der Ploeg, L.H., Schaeffer, J.M., Arena, J.P., 1994. Cloning of an avermectin-sensitive glutamate-gated chloride channel from Caenorhabditis elegans. Nature 371, 707–711. https://doi.org/10.1038/371707a0

Dalal, V., Tan, B.K., Xu, H., Cheng, W.W., 2025. Cryo-EM structures of a pentameric ligand-gated ion channel in liposomes. eLife 14, RP106728. https://doi.org/10.7554/eLife.106728

Dani, J.A., 2015. Neuronal Nicotinic Acetylcholine Receptor Structure and Function and Response to Nicotine. Int Rev Neurobiol 124, 3–19. https://doi.org/10.1016/bs.irn.2015.07.001

Elgoyhen, A.B., Johnson, D.S., Boulter, J., Vetter, D.E., Heinemann, S., 1994. α9: An acetylcholine receptor with novel pharmacological properties expressed in rat cochlear hair cells. Cell 79, 705–715. https://doi.org/10.1016/0092-8674(94)90555-X

Elgoyhen, A.B., Vetter, D.E., Katz, E., Rothlin, C.V., Heinemann, S.F., Boulter, J., 2001. α10: A determinant of nicotinic cholinergic receptor function in mammalian vestibular and cochlear mechanosensory hair cells. Proceedings of the National Academy of Sciences 98, 3501–3506. https://doi.org/10.1073/pnas.051622798

Goldschen-Ohm, M.P., Wagner, D.A., Jones, M.V., 2011. Three Arginines in the GABAA Receptor Binding Pocket Have Distinct Roles in the Formation and Stability of Agonist- versus Antagonist-Bound Complexes. Molecular Pharmacology 80, 647–656. https://doi.org/10.1124/mol.111.072033

Grudzinska, J., Schemm, R., Haeger, S., Nicke, A., Schmalzing, G., Betz, H., Laube, B., 2005. The β Subunit Determines the Ligand Binding Properties of Synaptic Glycine Receptors. Neuron 45, 727–739. https://doi.org/10.1016/j.neuron.2005.01.028

Grutter, T., Prado de Carvalho, L., Le Novère, N., Corringer, P.J., Edelstein, S., Changeux, J., 2003. An H-bond between two residues from different loops of the acetylcholine binding site contributes to the activation mechanism of nicotinic receptors. The EMBO Journal 22, 1990–2003. https://doi.org/10.1093/emboj/cdg197

Hardege, I., Morud, J., Courtney, A., Schafer, W.R., 2023. A Novel and Functionally Diverse Class of Acetylcholine-Gated Ion Channels. J Neurosci 43, 1111–1124. https://doi.org/10.1523/JNEUROSCI.1516-22.2022

566 Hughes, M.E., Mesoy, S.M., Capes, E., Lummis, S.C.R., 2020. Many Proline Residues in the
567 Extracellular Domain Contribute to Glycine Receptor Function. ACS Chem. Neurosci.
568 11, 2658–2665. https://doi.org/10.1021/acschemneuro.0c00320
569 Karlin, A., 2002. Emerging structure of the Nicotinic Acetylcholine receptors. Nat Rev
570 Neurosci 3, 102–114. https://doi.org/10.1038/nrn731
571 Katoh, K., Standley, D.M., 2013. MAFFT Multiple Sequence Alignment Software Version 7:
572 Improvements in Performance and Usability. Mol Biol Evol 30, 772–780.
573 https://doi.org/10.1093/molbev/mst010
574 Kouvatsos, N., Giastas, P., Chroni-Tzartou, D., Poulopoulou, C., Tzartos, S.J., 2016. Crystal
575 structure of a human neuronal nAChR extracellular domain in pentameric assembly:
576 Ligand-bound α2 homopentamer. Proceedings of the National Academy of Sciences
577 113, 9635–9640. https://doi.org/10.1073/pnas.1602619113
578 Lummis, S.C.R., Dougherty, D.A., 2022. Expression of Mutant Glycine Receptors in
579 Xenopus Oocytes Using Canonical and Non-Canonical Amino Acids Reveals Distinct
580 Roles of Conserved Proline Residues. Membranes 12, 1012.
581 https://doi.org/10.3390/membranes12101012
582 Lynagh, T., Pless, S.A., 2014. Principles of agonist recognition in Cys-loop receptors. Front.
583 Physiol. 5. https://doi.org/10.3389/fphys.2014.00160
584 Morales-Perez, C.L., Noviello, C.M., Hibbs, R.E., 2016. X-ray structure of the human α4β2
585 nicotinic receptor. Nature 538, 411–415. https://doi.org/10.1038/nature19785
586 Moroz, L.L., Romanova, D.Y., Kohn, A.B., 2021. Neural versus alternative integrative
587 systems: molecular insights into origins of neurotransmitters. Philosophical
588 Transactions of the Royal Society B: Biological Sciences 376, 20190762.
589 https://doi.org/10.1098/rstb.2019.0762
590 Morud, J., Hardege, I., Liu, H., Wu, T., Choi, M.-K., Basu, S., Zhang, Y., Schafer, W.R.,
591 2021. Deorphanization of novel biogenic amine-gated ion channels identifies a new
592 serotonin receptor for learning. Curr Biol 31, 4282-4292.e6.
593 https://doi.org/10.1016/j.cub.2021.07.036
594 Pan, J., Chen, Q., Willenbring, D., Yoshida, K., Tillman, T., Kashlan, O.B., Cohen, A., Kong,
595 X.-P., Xu, Y., Tang, P., 2012. Structure of the pentameric ligand-gated ion channel
596 ELIC cocrystallized with its competitive antagonist acetylcholine. Nat Commun 3,
597 714. https://doi.org/10.1038/ncomms1703
598 Parker, J.C., Sarkar, D., Quick, M.W., Lester, R.A.J., 2003. Interactions of atropine with
599 heterologously expressed and native α3 subunit-containing nicotinic acetylcholine
600 receptors. Br J Pharmacol 138, 801–810. https://doi.org/10.1038/sj.bjp.0705124

601 Peters, J.A., Malone, H.M., Lambert, J.J., 1990. Antagonism of 5-HT3 receptor mediated
602 currents in murine N1E-115 neuroblastoma cells by (+)-tubocurarine. Neuroscience
603 Letters 110, 107–112. https://doi.org/10.1016/0304-3940(90)90796-C
604 Puskar, N.L., Lester, H.A., Dougherty, D.A., 2012. Probing the Effects of Residues Located
605 Outside the Agonist Binding Site on Drug-Receptor Selectivity in the Nicotinic
606 Receptor. ACS Chem Biol 7, 841–846. https://doi.org/10.1021/cb200448j
607 Rahman, M.M., Basta, T., Teng, J., Lee, M., Worrell, B.T., Stowell, M.H.B., Hibbs, R.E.,
608 2022. Structural mechanism of muscle nicotinic receptor desensitization and block by
609 curare. Nat Struct Mol Biol 29, 386–394. https://doi.org/10.1038/s41594-022-00737-3
610 Ringstad, N., Abe, N., Horvitz, H.R., 2009. Ligand-gated chloride channels are receptors for
611 biogenic amines in C. elegans. Science 325, 96–100.
612 https://doi.org/10.1126/science.1169243
613 Sauguet, L., Shahsavar, A., Poitevin, F., Huon, C., Menny, A., Nemecz, À., Haouz, A.,
614 Changeux, J.-P., Corringer, P.-J., Delarue, M., 2014. Crystal structures of a
615 pentameric ligand-gated ion channel provide a mechanism for activation.
616 Proceedings of the National Academy of Sciences 111, 966–971.
617 https://doi.org/10.1073/pnas.1314997111
618 Spier, A.D., Lummis, S.C.R., 2000. The Role of Tryptophan Residues in the 5-
619 Hydroxytryptamine3 Receptor Ligand Binding Domain*. Journal of Biological
620 Chemistry 275, 5620–5625. https://doi.org/10.1074/jbc.275.8.5620
621 Su, J., Yu, Z., Yin, Z., Zhang, Z., Zhao, J., Meng, Y., Li, R., Gao, Y., Zhang, H., Yu, R., Zhao,
622 Y., 2025. Molecular insights into the α6β4 nicotinic acetylcholine receptor function
623 and ligand recognition. Nat Commun 16, 3153. https://doi.org/10.1038/s41467-025-
624 58333-0
625 Thompson, A.J., Lochner, M., Lummis, S.C.R., 2008. Loop B Is a Major Structural
626 Component of the 5-HT3 Receptor. Biophysical Journal 95, 5728–5736.
627 https://doi.org/10.1529/biophysj.108.135624
628 Tomaselli, G.F., McLaughlin, J.T., Jurman, M.E., Hawrot, E., Yellen, G., 1991. Mutations
629 affecting agonist sensitivity of the nicotinic acetylcholine receptor. Biophysical Journal
630 60, 721–727. https://doi.org/10.1016/S0006-3495(91)82102-6
631 Tomizawa, M., Maltby, D., Talley, T.T., Durkin, K.A., Medzihradszky, K.F., Burlingame, A.L.,
632 Taylor, P., Casida, J.E., 2008. Atypical nicotinic agonist bound conformations
633 conferring subtype selectivity. Proc Natl Acad Sci U S A 105, 1728–1732.
634 https://doi.org/10.1073/pnas.0711724105
635 Unwin, N., 2003. Structure and action of the nicotinic acetylcholine receptor explored by
636 electron microscopy. FEBS Lett 555, 91–95. https://doi.org/10.1016/s0014-
637 5793(03)01084-6

638 Yan, D., Pedersen, S.E., White, M.M., 1998. Interaction of D-tubocurarine analogs with the
639 5HT3 receptor. Neuropharmacology 37, 251–257. https://doi.org/10.1016/s0028-
640 3908(98)00010-0
641 Zwart, R., Vijverberg, H.P.M., 1998. Four Pharmacologically Distinct Subtypes of α4β2
642 Nicotinic Acetylcholine Receptor Expressed in Xenopus laevisOocytes. Molecular
643 Pharmacology 54, 1124–1131. https://doi.org/10.1124/mol.54.6.1124
644 Zwart, R., Vijverberg, H.P.M., 1997. Potentiation and Inhibition of Neuronal Nicotinic
645 Receptors by Atropine: Competitive and Noncompetitive Effects. Molecular
646 Pharmacology 52, 886–895. https://doi.org/10.1124/mol.52.5.886
647

648

649 **Supplementary data**

650 Table S 1 Protein sequences used for alignments.

Name	**Protein Sequence**
O_sinensis_DopC1	MNYRLYIAMTLMKDIRILMSAFHLLMGASIALCDENEYRLVRDLMKNYNKQV RPSSNFSEALNVTFGVALAQIIDVDEKDQIITTNCWINQNWIDYKLQWDPIKY GNVSVIRLPFSDIWRPDILLYNNADVKAFESSISTNVIVTSEGNVTWLSMVIFK SSCSIDVKFFPFDEQNCSMEFASWTYDAYQVNILTNGEDNGDMSNYIENSE WSLIGFQQKRHVVRFSCCEEPYIIIHYHILIKRRPLFYLFNMVMPCILITLVALLG FYMPSDSGEKISMGITTLLSMTVFLMIVAEKMPPTSDVLPLIGLYYGITIAIVSF ATGMTVLTLNIHHKGTRGYEVPMILKKICFGVVAKILFIKLEVPLGSKESMPAA PVADYYRRFDTDKLPENGRLSPRFIRKLNPSASATASETFERQFMRVLQKVY QTIERNEMRLAEQDRRDLIKQEWQQLALIIDRVLLLIFLGLTITVTLTVFFQGP-- ---------- ----------
O_sinensis_DopC2	MEFWASITLTIFSLCLPSSSADDVELSLVNRLLKNYDKRVRPSLNSSEAINVTF GVALAQIIDVDERNQILTTNCWLNQVWLDVNLRWDPDKYNGIKVVRIPFTDV WKPDILLYNNADVTSYFSSLSSNVIVTSEGNVTWLSMVIFKSSCRIDVRYFPF DEQNCSMQFASWTYDGFQLQLRMNSEEGDISNYIRNSEWVLIKLHVEWNLV YYSCCIEPYPDITYYIQIRRRPLFYVFNMILPCILITLVALLGFYIPSDSGEKVTM GITTLLSMTVFMMLVAENMPPTSDVLPLIGIYYGITISIVSFATAMTVFTLNIHH KGARGHEVPIIIKKICFGILAKIFCMRLEKPNNKSSNVAHLSDMSSSSEIPEMF VPCSSQSNSSYIRFKLSSQEESDQNAKPLLEMNPTLSQQQSMIRETRFHGD LETSNGGILSPRFSRLRGLQSRLTSPTHSSDDFERQFKRVLTKVYQTIERNEI

	RLAEQDRRDVIKLEWQQVAQIVDRLFLTIFVCVTILITCIVMFKAPHSTESLIS---------- ----------
A_californica_DopC1	MADGINLILSLLVLASCAVMWTRGDPNEYRLVRDLMKGYDKRIRPSLNHTDS LNVTFGLALVQIIDVDEKNQILTTNCWLNQIWTDYNLRWDPAKYGGIKVLRLP YDEVWKPDILLHNNAEVSTFVSSTSSNLIVTNDGNVTWFSMVIFKSSCSINVR YFPFDAQNCSMQFASWSYDGYQVNLIMNTEKGDTSNYIHNSEWELIYLQVE RTVRIFSCCEEPYPDIHFHILIKRRPLFYIFNMILPCILITLVALLGFYIPSDSGEK VTMGITTLLSMTVFMMLVTENMPPTSDVLPLIGIYYGMTIFIVSFATAMTVFTL NIHHKGSRGKAVPMVIKKICFDFLAKMFCMKVDTWDEKHFTPDCNGTPGGA SNYIRFKVANQQDTDQLNMELKQTHEMSPLNRVELPLDSESFQSNGAVPRA FTSFRSSNGNGGSSSEQQNTELTGFEAYFSRVLQRVYQTIERNDIRLAEQDK REGIKLEWQQVAQITDRLLLTCFVLVTLTITGVVLLASPASVKV---------- ----------
D_magna_DopC1	MLRSHKMTQRIWIAFVTVLAIPGNRGDDGEYTRPIVSHEYRLIQHLMANYDR SVRPSRNAAEPLNITFGLALTQIIDVDERNQILTTNCWMNQMWTDYSLVWNV SEFGGIRVVRIPADKVWKSDIILYNNADSEYNSALLSTNVIVTHDGNLTWLSS AIFKSSCGINVEYFPFDEQKCSMKFSSWTYDGLQVNLLNQAEEGDLSNYVP NGEWDLIDLVVERNVVFYSCCEEPYPDITFHIVLRRRPLFYVFNLILPCVLITGI ALMSFYMPSDSGEKVTLGITTLLSMTVFLMVIGESMPPTSEKLPLIGLYYGVTI SLVSFATGLSVVTLNIHHRGMRGRGVPPMVKKIVFGVLAKLLFIQLDIAEGCS CSTKAKEFQQNNQFEMNERFNVDIGDSLKNESNGSLPHRLVVVFVAAAWFH VRQSSFGANSGLINNATSNIGPTDSFERQFLRVLNKVYQHIERSEARLADQD RKDAIKLEWQQVALVIDRFLLWIFIIATVAATFGILYMSPHSRLFSM---------- ----------
D_magna_DopC2	MESKAMSPQSVSVRTAGRLLLSLGLFVLLPEAVHSDLNEYRLLRHLMENYDS NARPVANSTKALQVIFGMSLHLLIDVDERNQILTTNCWLTQKWNDSHLTWNA SDYGGIHVVRIPYHRVWRPDIILYNNADAQYTSSVINTNVIVSDNGEVVWLSH GIFRSSCDINVEYFPFDLQSCKMKWASWTYDGFQIDLKKQTDEGDVSNYQT NGEFDLVDFEAIHHEEYYSCCPEPYPDITYVIKMRRRPLFYVFNLILPCLLINGI ALLVFYVPSESGEKVTLGISSLLSMTVFLMTIRESLPPTEKTPLISLYYGVSICL VSFASGLSVVTLNLHHRGLRGTEVPYIMRRIILGGLARLVFLRFDVDKRHSPA STPTSAPAGEPSSSHSGDPIPASRLASRFEESPTKTCASGDPRCTCGKSRNI NQRGRHQPVGVSATRSSGWYSTPVNGGPSCSRNSQERLRLRLQELEPRAT DVYLDPEFSDKFQSAELDFLGIGPPSPKFYSRRVPSTSKAPHFQQQQQPLI NPESASGSSSAEIGGGFGLLSQGSIYEQRLTELMARVSTAVERNENRLEEQ DRREAIALEWKQLALVCDRILLLTFVIITTVATCVVLTSSPYGP

A_mellifera_DopC1	MIPTSYKQPVCLTFVSALFETPARIFLGIEVRWSRGSAGFRVEIARWLKSIGY QSRTGGLAFKWSINSMSPLVLFFHYGVLAIIFGNGFGDEHEYRLTKYLLDGY DAGVRPAENSSQPLAVVFGLSLHHIIDVDEKNQILTTNCWVTQIWTDHHLKW NASEFAGIRVIRVPYNRVWRPDTILYNNADPQYSSAVINTNVIVSHTGEVVWL SHGIFRSSCDIDVEFFPFDEQRCVLKWASWTYDGYQLELEKQSEQGDVSNY QANGEFDLVNFSARRNVEYYSCCPEPYPDITYEIRLRRRPMFYVFNLILPCILI NSVALLVFYVPSESGEKVTLGISALLSMTVFLMTIRESLPPTEKTPLISLYYGV SICLVTFASALAVVTLNLHHRGVRGTRVPGIVRSLVLDKLARIVLLNFQEERRS EPVEPPRRKNNCPLHCKPELGQSQSSPKFVARREESNSSSPSLDLGKEGGL EAQWSRVLGRVHATIERNEKRLAEQDRRERMEFDWKQVALVSDRALLCVF FLTTIVSTTVILCGSPPSANIAKEG----------
H_sapiens_ACHA9	MNWSHSCISFCWIYFAASRLRAAETADGKYAQKLFNDLFEDYSNALRPVED TDKVLNVTLQITLSQIKDMDERNQILTAYLWIRQIWHDAYLTWDRDQYDGLD SIRIPSDLVWRPDIVLYNKADDESSEPVNTNVVLRYDGLITWDAPAITKSSCV VDVTYFPFDNQQCNLTFGSWTYNGNQVDIFNALDSGDLSDFIEDVEWEVHG MPAVKNVISYGCCSEPYPDVTFTLLLKRRSSFYIVNLLIPCVLISFLAPLSFYLP AASGEKVSLGVTILLAMTVFQLMVAEIMPASENVPLIGKYYIATMALITASTALT IMVMNIHFCGAEARPVPHWARVVILKYMSRVLFVYDVGESCLSPHHSRERD HLTKVYSKLPESNLKAARNKDLSRKKDMNKRLKNDLGCQGKNPQEAESYCA QYKVLTRNIEYIAKCLKDHKATNSKGSEWKKVAKVIDRFFMWIFFIMVFVMTIL IIARAD
G_gallus_ACHA9	MKRNNLSSFYVSLWLLFTATMLQAVESAKGKYAQMLFNELFEDYSNALRPV EDTDKVLNVTLQITLSQIKDMDERNQILTAYLWIRQSWYDAYLKWDKDKYDG LDSIRIPSNLVWRPDIVLYNKADDDFSEPVNTNVVLRYDGKITWDAPAITKSS CVVDVSYFPFDSQQCNLTFGSWTYNGNQVDIINSLDSGDLSDFVEDVEWEI HGMPAVKNVITYGCCSEPYPDVTFTLILKRKSSFYIFNLLLPCILISFLAPLGFY LPADSGEKVSLGVTVLLALTVFQLMVAEIMPPSENVPLIGKYYIATMTMITAST ALTIIIMNVHHCGSEAKPVPQWARVVILDYMSKIFFVYDVGENCTSPRREKEQ EHRLEGGDMCRGGDGKSHLSSRNDDSDLKENLNGNWNKSFGVHGENVRE NVNCCSCYKMLIKNIEYIANCVRDHKANRAKGIEWKKVAKVMDRFFMWIFFI MVFFMSVLIIGKAA
G_gallus_ACH10	MGSAPLPACLLALSLAGTVLAPGCGAAQGRLAHKLLHDLFANYSSALRPAED TERALNVTLQVTLSQIIDMDERNQVLTSYLWVRQAWLDAHLAWDKDAYGGI DSIRIPSSYVWRPDIVLYNNADERFGGSMETNVVLRSDGHIMWDSPAITKSS CKVDVSYFPFDGQQCRLTFGSWTYNGNQIDLRNLLDTGDLTDFVENVEWEV

	LGMPATRNVVTYGCCSEPYPDVTYTLLLRRRASFYIFNLLLPCVMISFLAPLG FYLPADSGEKVSLGVTVLLALTVFQLLVAESMPPSESVPLIGKYYIATMTMITA STALTIFIMNIHHCGPGARPVPPWARRLILHHLARALCVCEVGESCGRPQRE GTGGMGPRDPPGEGVEPGLCPRSRCLCHHHAVLSSVGYIAGVFRRHRTAQ RRAAEWKKVAKVMDRFFMWVFFLMVFLMSVLVIGKAA
H_sapiens_ ACH10	MGLRSHHLSLGLLLLFLLPAECLGAEGRLALKLFRDLFANYTSALRPVADTDQ TLNVTLEVTLSQIIDMDERNQVLTLYLWIRQEWTDAYLRWDPNAYGGLDAIRI PSSLVWRPDIVLYNKADAQPPGSASTNVVLRHDGAVRWDAPAITRSSCRVD VAAFPFDAQHCGLTFGSWTHGGHQLDVRPRGAAASLADFVENVEWRVLG MPARRRVLTYGCCSEPYPDVTFTLLLRRRAAAYVCNLLLPCVLISLLAPLAFH LPADSGEKVSLGVTVLLALTVFQLLLAESMPPAESVPLIGKYYMATMTMVTFS TALTILIMNLHYCGPSVRPVPAWARALLLGHLARGLCVRERGEPCGQSRPPE LSPSPQSPEGGAGPPAGPCHEPRCLCRQEALLHHVATIANTFRSHRAAQRC HEDWKRLARVMDRFFLAIFFSMALVMSLLVLVQAL
H_sapiens_ ACHA7	MRCSPGGVWLALAASLLHVSLQGEFQRKLYKELVKNYNPLERPVANDSQPL TVYFSLSLLQIMDVDEKNQVLTTNIWLQMSWTDHYLQWNVSEYPGVKTVRF PDGQIWKPDILLYNSADERFDATFHTNVLVNSSGHCQYLPPGIFKSSCYIDVR WFPFDVQHCKLKFGSWSYGGWSLDLQMQEADISGYIPNGEWDLVGIPGKR SERFYECCKEPYPDVTFTVTMRRRTLYYGLNLLIPCVLISALALLVFLLPADSG EKISLGITVLLSLTVFMLLVAEIMPATSDSVPLIAQYFASTMIIVGLSVVVTVIVL QYHHHDPDGGKMPKWTRVILLNWCAWFLRMKRPGEDKVRPACQHKQRRC SLASVEMSAVAPPPASNGNLLYIGFRGLDGVHCVPTPDSGVVCGRMACSPT HDEHLLHGGQPPEGDPDLAKILEEVRYIANRFRCQDESEAVCSEWKFAACV VDRLCLMAFSVFTIICTIGILMSAPNFVEAVSKDFA
H_sapiens_ ACHA3	MGSGPLSLPLALSPPRLLLLLLLSLLPVARASEAEHRLFERLFEDYNEIIRPVA NVSDPVIIHFEVSMSQLVKVDEVNQIMETNLWLKQIWNDYKLKWNPSDYGG AEFMRVPAQKIWKPDIVLYNNAVGDFQVDDKTKALLKYTGEVTWIPPAIFKSS CKIDVTYFPFDYQNCTMKFGSWSYDKAKIDLVLIGSSMNLKDYWESGEWAII KAPGYKHDIKYNCCEEIYPDITYSLYIRRLPLFYTINLIIPCLLISFLTVLVFYLPS DCGEKVTLCISVLLSLTVFLLVITETIPSTSLVIPLIGEYLLFTMIFVTLSIVITVFV LNVHYRTPTTHTMPSWVKTVFLNLLPRVMFMTRPTSNEGNAQKPRPLYGAE LSNLNCFSRAESKGCKEGYPCQDGMCGYCHHRRIKISNFSANLTRSSSSES VDAVLSLSALSPEIKEAIQSVKYIAENMKAQNEAKEIQDDWKYVAMVIDRIFL WVFTLVCILGTAGLFLQPLMAREDA
H_sapiens_ ACHA4	MELGGPGAPRLLPPLLLLLGTGLLRASSHVETRAHAEERLLKKLFSGYNKWS RPVANISDVVLVRFGLSIAQLIDVDEKNQMMTTNVWVKQEWHDYKLRWDPA

	DYENVTSIRIPSELIWRPDIVLYNNADGDFAVTHLTKAHLFHDGRVQWTPPAI YKSSCSIDVTFFPFDQQNCTMKFGSWTYDKAKIDLVNMHSRVDQLDFWESG EWVIVDAVGTYNTRKYECCAEIYPDITYAFVIRRLPLFYTINLIIPCLLISCLTVLV FYLPSECGEKITLCISVLLSLTVFLLLITEIIPSTSLVIPLIGEYLLFTMIFVTLSIVIT VFVLNVHHRSPRTHTMPTWVRRVFLDIVPRLLLMKRPSVVKDNCRRLIESMH KMASAPRFWPEPEGEPPATSGTQSLHPPSPSFCVPLDVPAEPGPSCKSPS DQLPPQQPLEAEKASPHPSPGPCRPPHGTQAPGLAKARSLSVQHMSSPGE AVEGGVRCRSRSIQYCVPRDDAAPEADGQAAGALASRNTHSAELPPPDQP SPCKCTCKKEPSSVSPSATVKTRSTKAPPPHLPLSPALTRAVEGVQYIADHL KAEDTDFSVKEDWKYVAMVIDRIFLWMFIIVCLLGTVGLFLPPWLAGMI
C_elegans_ UNC-29	MRTNRLSWILVLSVVIFLVIINTINASDDEERLMVDVFRGYNSLIQPVRNSSEL PLIVKMALQLVLLINVDEKDQVMHTNVWLTLQWHDFQMKWNPVNYGEIKQIR VSPDKVWLPDIVLFNNADGNYEVSFMCNVVINHKGDMLWVPPAIYKSSCIID VEFFPFDEQVCTLVFGSWTYNENEIKLEFVQAELVDVSEYSASSIWDVIDVPA SLVNKRSRIEFQVRIRRKTLFYTVVLIIPTVLMAFLSMAVFFLPTDSGEKITLTIS VLLSIVVFLLLVSKILPPTSSTIPLMAKYLLLTFVLNVITILVTVIIINVYFRGPRTH RMPQWVRVVFLQFLPKLVCMKRPKSASERSAVRSGMAQLPGVGQFTLSPS AHHPLCPSADDRTTTIRNTASNETSAYYPLSTDALRAIDAIEYITEHLKRDEQH KSFRDDWKYVAMIIDRLLLYVFFGITVGGTCGILFSAPHVFQRIDQQEMLDRL KEKYDTASNIP
D_chrysanth emi_ELIC	APADNAADARPVDVSVSIFINKIYGVNTLEQTYKVDGYIVAQWTGKPRKTPG DKPLIVENTQIERWINNGLWVPALEFINVVGSPDTGNKRLMLFPDGRVIYNAR FLGSFSNDMDFRLFPFDRQQFVLELEPFSYNNQQLRFSDIQVYTENIDNEEID EWWIRKASTHISDIRYDHLSSVQPNQNEFSRITVRIDAVRNPSYYLWSFILPL GLIIAASWSVFWLESFSERLQTSFTLMLTVVAYAFYTSNILPRLPYTTVIDQMII AGYGSIFAAILLIIFAHHRQAMGVEDDLLIQRCRLAFPLGFLAIGCVLVIRGITL
H_sapiens_ 5HT3A	MLLWVQQALLALLLPTLLAQGEARRSRNTTRPALLRLSDYLLTNYRKGVRPV RDWRKPTTVSIDVIVYAILNVDEKNQVLTTYIWYRQYWTDEFLQWNPEDFDN ITKLSIPTDSIWVPDILINEFVDVGKSPNIPYVYIRHQGEVQNYKPLQVVTACSL DIYNFPFDVQNCSLTFTSWLHTIQDINISLWRLPEKVKSDRSVFMNQGEWEL LGVLPYFREFSMESSNYYAEMKFYVVIRRRPLFYVVSLLLPSIFLMVMDIVGF YLPPNSGERVSFKITLLLGYSVFLIIVSDTLPATAIGTPLIGVYFVVCMALLVISL AETIFIVRLVHKQDLQQPVPAWLRHLVLERIAWLLCLREQSTSQRPPATSQAT KTDDCSAMGNHCSHMGGPQDFEKSPRDRCSPPPPPREASLAVCGLLQELS SIRQFLEKRDEIREVARDWLRVGSVLDKLLFHIYLLAVLAYSITLVMLWSIWQY A

H_spaiens_ACHB2	MARRCGPVALLLGFGLLRLCSGVWGTDTEERLVEHLLDPSRYNKLIRPATN GSELVTVQLMVSLAQLISVHEREQIMTTNVWLTQEWEDYRLTWKPEEFDNM KKVRLPSKHIWLPDVVLYNNADGMYEVSFYSNAVVSYDGSIFWLPPAIYKSA CKIEVKHFPFDQQNCTMKFRSWTYDRTEIDLVLKSEVASLDDFTPSGEWDIV ALPGRRNENPDDSTYVDITYDFIIRRKPLFYTINLIIPCVLITSLAILVFYLPSDCG EKMTLCISVLLALTVFLLLISKIVPPTSLDVPLVGKYLMFTMVLVTFSIVTSVCVL NVHHRSPTTHTMAPWVKVVFLEKLPALLFMQQPRHHCARQRLRLRRRQRE REGAGALFFREAPGADSCTCFVNRASVQGLAGAFGAEPAPVAGPGRSGEP CGCGLREAVDGVRFIADHMRSEDDDQSVSEDWKYVAMVIDRLFLWIFVFVC VFGTIGMFLQPLFQNYTTTTFLHSDHSAPSSK
H_sapines_ACHB4	MRRAPSLVLFFLVALCGRGNCRVANAEEKLMDDLLNKTRYNNLIRPATSSSQ LISIKLQLSLAQLISVNEREQIMTTNVWLKQEWTDYRLTWNSSRYEGVNILRIP AKRIWLPDIVLYNNADGTYEVSVYTNLIVRSNGSVLWLPPAIYKSACKIEVKYF PFDQQNCTLKFRSWTYDHTEIDMVLMTPTASMDDFTPSGEWDIVALPGRRT VNPQDPSYVDVTYDFIIKRKPLFYTINLIIPCVLTTLLAILVFYLPSDCGEKMTLC ISVLLALTFFLLLISKIVPPTSLDVPLIGKYLMFTMVLVTFSIVTSVCVLNVHHRS PSTHTMAPWVKRCFLHKLPTFLFMKRPGPDSSPARAFPPSKSCVTKPEATA TSTSPSNFYGNSMYFVNPASAASKSPAGSTPVAIPRDFWLRSSGRFRQDVQ EALEGVSFIAQHMKNDDEDQSVVEDWKYVAMVVDRLFLWVFMFVCVLGTV GLFLPPLFQTHAASEGPYAAQRD
C_elegans_LGC-53	MIISYLARIVLLLPELSSGDTDRLAEIAANQEHSIQLDQMPPDRTFHYPNIPSS QHDRRREGGKRKKFRKERLDEPCTAINETLRKNLLQELFDDSYDKNNLPSA NSTEVIVELTVQSITEISEFSSSFKADVWFSQIWRDPRLDFSDRNYCLKNISLA SHKLPTMWSPNVCFVNSKKVEIHASPSQNILLLIFPNGTVWLNFRVSLTGPC KLDLTYFPMDRQSCNLVFESYSYNTAEVRIVWRDWDAVTIPDPDSKNLPDFE LVNIEHMNATLVYTAGLWDQLEVKFTFRRLYGYYVLQAYMPTYLSVFISWIAF WIDTKALPARITLGVSSLMALTFQFGNIVKNLPRVSYVKALDIWMFGCVGFIFL SLVELAVVGFADKLEAKRRRHNRCKEQLMMRSDSEQQWLSRLSGQRPQVS ETNSDATHTIQINDGNGNVRRRKSEEKRQKLLLQMESPMFVNGEKIDEISAK LFPLLFTAFNIFYWFYYIGMSGGFF
C_elegans_LGC-52	MIYSIQALFIETILMSARIHDVTYQHIEDFTCDDIGLSSLSGAKATDLARILMTNY SRNALPEPAPVKVEVEITIQDISDISAITGTFTIDYWISAIWNDKRLAFSHLDPC RKNLSLDHDMEPKLWSPNVCIVNSKSTKVHDSPKPNILLMIFPNGTIWLNYRI RSEAPCQMNLRNFPLDSIRCSLVFESYSYNAADVELQWLEWSPVSTVRNDY NLPDFRMTNITYGSVTEAYTAGMWHRLSVSIHFERLYGFYILQMYLPTYISVFI SWIAFWMDTKALPARITLSVSSLMALTFQFGNIVKSLPKASYVKAIDIWMFSC

	VGFIFFSLIELAIVAYNDKMHDQRLREVRCSVGNLNSNGIGQYNSTTRRSFVE LSARRAKGSELGASIDRVASMLFPTMFALFNLVYWAYYLTTSMNPVYT
D_melanogaster_HisCl1	MQSPTSKLVEFRCLIALAIYLHALEQSIQHCHCVHGYRNNTESAELVSHYESS LSLPDILPIPSKTYDKNRAPKLLGQPTVVYFHVTVLSLDSINEESMTYVTDIFLA QSWRDPRLRLPENMSEQYRILDVDWLHSIWRPDCFFKNAKKVTFHEMSIPN HYLWLYHDKTLLYMSKLTLVLSCAMKFESYPHDTQICSMMIESLSHTVEDLV FIWNMTDPLVVNTEIELPQLDISNNYTTDCTIEYSTGNFTCLAIVFNLRRRLGY HLFHTYIPSALIVVMSWISFWIKPEAIPARVTLGVTSLLTLATQNTQSQQSLPP VSYVKAIDVWMSSCSVFVFLSLMEFAVVNNFMGPVATKAMKGYSDENISDL DDLKSALQHHRESIIEPQYDTFCHGHATAIYIDKFSRFFFPFSFFILNIVYWTTF L
H_sapiens_GBRA1	MRKSPGLSDCLWAWILLLSTLTGRSYGQPSLQDELKDNTTVFTRILDRLLDG YDNRLRPGLGERVTEVKTDIFVTSFGPVSDHDMEYTIDVFFRQSWKDERLKF KGPMTVLRLNNLMASKIWTPDTFFHNGKKSVAHNMTMPNKLLRITEDGTLLY TMRLTVRAECPMHLEDFPMDAHACPLKFGSYAYTRAEVVYEWTREPARSV VVAEDGSRLNQYDLLGQTVDSGIVQSSTGEYVVMTTHFHLKRKIGYFVIQTY LPCIMTVILSQVSFWLNRESVPARTVFGVTTVLTMTTLSISARNSLPKVAYAT AMDWFIAVCYAFVFSALIEFATVNYFTKRGYAWDGKSVVPEKPKKVKDPLIK KNNTYAPTATSYTPNLARGDPGLATIAKSATIEPKEVKPETKPPEPKKTFNSV SKIDRLSRIAFPLLFGIFNLVYWATYLNREPQLKAPTPHQ

651

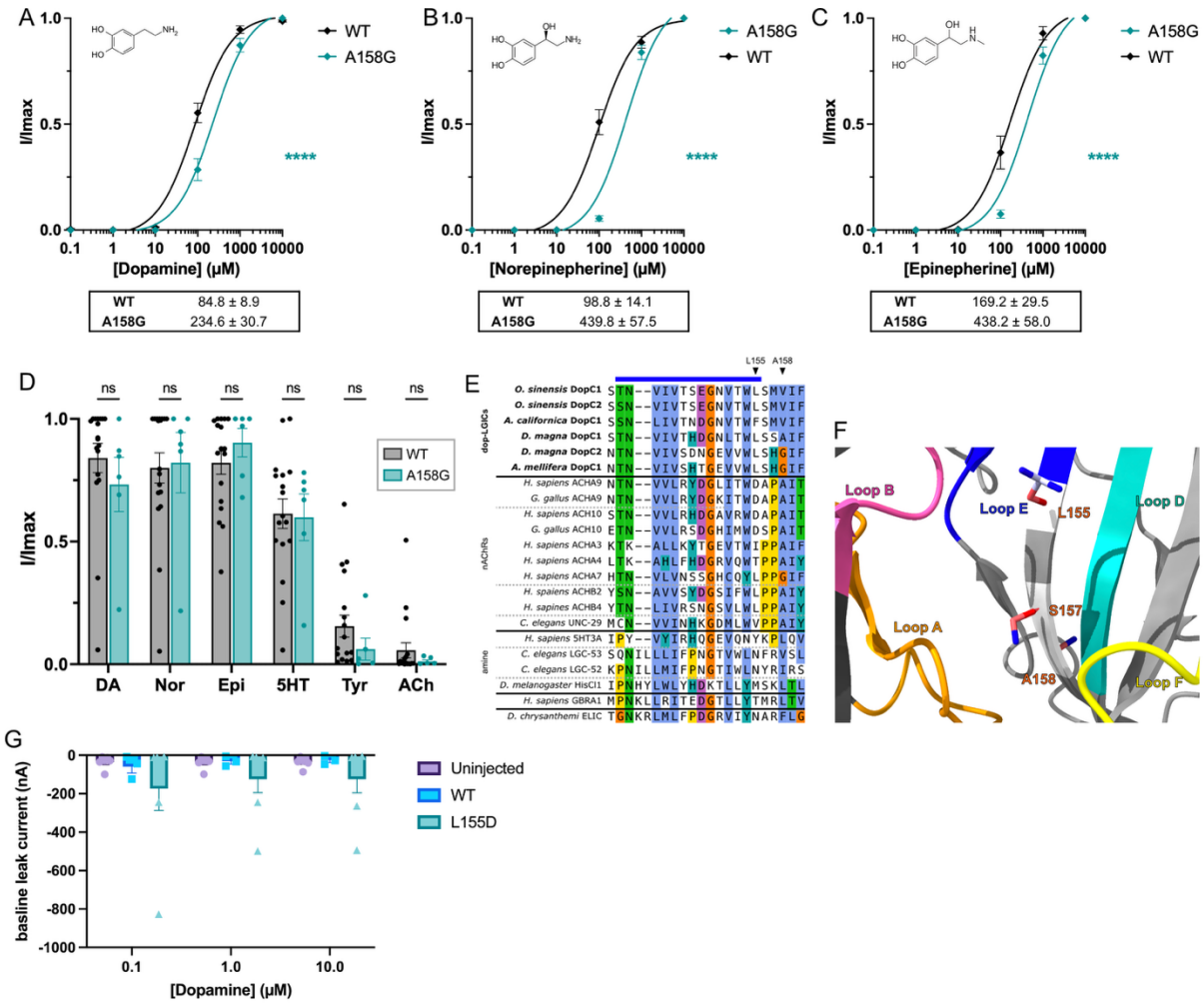

Figure S 1 The A158G mutation in Loop E of a *D. magna* dop-LGIC decreases catecholamine sensitivity.

A-C. Dose response curves for dopamine (A), norepinephrine (B) and epinephrine (C) in wild-type and A158G Dm-DopC1 expressing *Xenopus* oocytes. Current normalized by I/Imax. EC_{50} values (± SEM) shown below each plot. **** = P<0.0001, ns = not significant calculated by sum of squares F test. WT: *n* = 24 (dopamine), 12 (norepinephrine), 11 (epinephrine); A158G: *n* = 10 (dopamine), 11 (norepinephrine), 10 (epinephrine). **D.** Relative maximum I/Imax currents of *Xenopus* oocytes expressing wild-type and A158G Dm-DopC1, perfused for 10 s with 1 mM each: dopamine (DA), norepinephrine (Nor), epinephrine (Epi), serotonin (5HT), tyramine (Tyr), and acetylcholine (ACh). WT: *n* = 18 (dopamine, norepinephrine, ACh, tyramine), 17 (epinephrine, serotonin); A158G: *n* = 6 per agonist. ns = not significant by one-way ANOVA and a Fisher's LSD. **E.** Sequence alignment of the loop E region. Residues A158 and L155 are indicated by arrows, loop E is highlighted by the blue bar. **F.** AlphaFold2 model of the loop E (blue) region of Dm-DopC1 with A158 and L155 relative to loop B (pink), loop C (green), loop F (yellow), loop A (orange) and loop D (turquoise) at the ligand-binding site. **G.**

668 Baseline currents in uninjected oocytes or oocytes expressing WT or L155D Dm-DopC1.
669 Baseline currents measured 5s before agonist application. Error bars represent SEM, *n* = 3
670 (WT), 6 (uninjected), 7 (L155D).

671

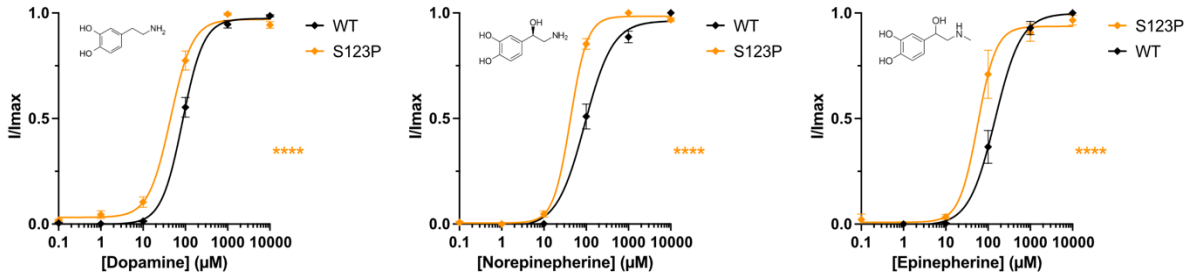

	Hillslope
WT	1.74 ± 0.50
S123P	1.67 ± 0.22

	Hillslope
WT	1.31 ± 0.30
S123P	2.16 ± 0.19

	Hillslope
WT	1.40 ± 0.38
S123P	1.99 ± 1.14

672

673 **Figure S 2 S123P exhibits a steeper Hill slope than wild type for norepinephrine.**

674 **A-C.** Dose response curves for dopamine (A), norepinephrine (B) and epinephrine (C) in wild-
675 type and S123P Dm-DopC1 expressing *Xenopus* oocytes. Current normalized by I/Imax. Hill
676 slope values are shown underneath each plot with SEM, calculated with a 4-parameter curve.
677 WT: *n* = 24 (dopamine), 12 (norepinephrine), 11 (epinephrine); S123P: n = 12, (dopamine), 4
678 (norepinephrine) and 8 (epinephrine).

679

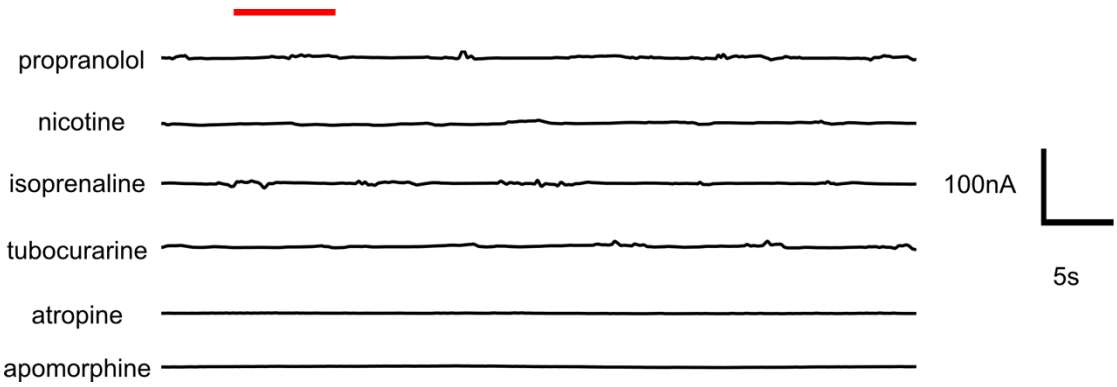

680

681 **Figure S 3 Continuous traces of Dm-DopC1 oocytes exposed to a panel of compounds.**
682 Red bar indicates application of 100μM compound.

683